Deuterium and ^{37}Chlorine Rich Fluids on the Surface of Mars: Evidence from the Enriched Basaltic Shergottite Northwest Africa 8657

JGR Planets

RESEARCH ARTICLE
10.1029/2020JE006537

Key Points:
- First report of H and Cl isotopic systematics of apatite from the Martian meteorite NWA 8657
- NWA 8657 apatite has the highest reported δD value (up to 6,509‰) of any phosphates in Martian meteorites
- The H and Cl isotopic compositions of apatite in NWA 8657 imply D- and ^{37}Cl-rich fluids on surface of Mars

Supporting Information:
- Supporting Information S1

Correspondence to:
S. Hu,
husen@mail.iggcas.ac.cn

Citation:
Hu, S., Lin, Y., Anand, M., Franchi, I. A., Zhao, X., Zhang, J., et al. (2020). Deuterium and ^{37}chlorine rich fluids on the surface of Mars: Evidence from the enriched basaltic shergottite Northwest Africa 8657. *Journal of Geophysical Research: Planets*, *125*, e2020JE006537. https://doi.org/10.1029/2020JE006537

Received 11 JUN 2020
Accepted 26 AUG 2020

Deuterium and ^{37}Chlorine Rich Fluids on the Surface of Mars: Evidence From the Enriched Basaltic Shergottite Northwest Africa 8657

S. Hu[1,2,3], Y. Lin[1,2], M. Anand[3,4], I. A. Franchi[3], X. Zhao[3], J. Zhang[1,2], J. Hao[1,2], T. Zhang[1,2], W. Yang[1,2], and H. Changela[1,5,6]

[1]Key Laboratory of Earth and Planetary Physics, Institute of Geology and Geophysics, Chinese Academy of Sciences, Beijing, China, [2]Innovation Academy for Earth Science, Chinese Academy of Sciences, Beijing, China, [3]School of Physics Sciences, The Open University, Milton Keynes, UK, [4]Department of Earth Sciences, The Natural History Museum, London, UK, [5]Qianxuesen Laboratory of Space Technology, Chinese Academy of Space Technology, Beijing, China, [6]Department of Earth and Planetary Sciences, University of New Mexico, Albuquerque, NM, USA

Abstract Apatite, a major hydrous mineral in Martian meteorites, has the potential to reveal history of volatiles on Mars. Here we report the H and Cl isotopic systematics of apatite from the enriched basaltic shergottite Northwest Africa (NWA) 8657 to better understand the processes influencing volatiles at or near the Martian (sub)surface. The apatite in NWA 8657 has the highest reported δD value (up to 6,509‰) of any phosphates in Martian meteorites. The positive correlation between the H_2O contents (72–2,251 ppm) and δD values (3,965–6,509‰) as well as between the Cl contents (1.28–6.17wt%) and δ^{37}Cl values (−1.7–4.0‰) in NWA 8657 apatite are consistent with mixing between volatiles derived from the Martian mantle and meteoric water/fluid. The D- and ^{37}Cl-enrichment of apatite in NWA 8657 implies isotopic exchange with subsurficial fluids during postcrystallization hydrothermal event(s).

Plain Language Summary Mars was probably a wet and warm world during its earliest geological history, supported by many lines of evidence. Present-day Mars is cold and arid although recent remote sensing data support the existence of subsurface glaciers and seasonal fluid activities at some locations. In this study, our aim was to use ground truth about the potential water-rock interaction on or near-surface environments on recent Mars via measuring the H and Cl isotopic compositions of apatite from a geologically young meteorite from Mars: the enriched basaltic shergottite Northwest Africa (NWA) 8657. The petrography and mineral chemistry of apatite and other associated phases, for example, merrillite, maskelynite, mesostasis, and pyroxene, were documented prior to in situ H and Cl isotopes analysis. The water contents of apatite, merrillite, maskelynite, mesostasis, and pyroxene are positively correlated with the δD values. All of the data sets can be reconciled in terms of mixing between two end-members, a D-poor (~0‰) mantle reservoir and a D-rich (5,920 ± 500‰) near-surface/underground water reservoir. Moreover, apatite in NWA 8657 displays ^{37}Cl-enriched (~1 ± 1‰ in average) characteristics. These signatures are consistent with D- and ^{37}Cl-rich fluid-assisted isotopic exchange in recent near-surface environment on Mars.

1. Introduction

Early Mars probably had liquid water that formed by volcanic degassing (McCubbin et al., 2010; McSween et al., 2001) of volatiles, which were originally delivered by early-formed planetesimals (Elkins-Tanton et al., 2005) in the first hundreds of million years of its history (Carr, 1987). However, the paleoclimate of Mars gradually changed from warm and wet to cold, and arid conditions attributed to the dissipation of internal energy and the disappearance of a magnetic field at ~4 Ga ago (Ehlmann et al., 2011). Any atmospheric water present on Mars at that time was subsequently lost via the action of solar wind (Jakosky et al., 2015; Wei et al., 2014). This led to the hydrogen isotopic composition of the Mars' atmosphere becoming progressively enriched in D by the preferential loss of H compared to D (Owen et al., 1988). Therefore, throughout Mars' geological history, the H isotopic composition of the surficial (or underground, hereafter we use surficial in simplicity) water reservoir would have equilibrated with Mars' atmosphere via a water cycle (Jakosky et al., 1997). Measurements from astronomical observations (Owen et al., 1988; Villanueva et al., 2015) and

NASA's Mars Science Laboratory (MSL) (Leshin et al., 2013; Webster et al., 2013) support that Mars' atmosphere and sedimentary materials are highly enriched in D relative to the Earth, Moon, 4 Vesta, and chondrites (Hallis, 2017; Robert et al., 2000). Similarly, the study of Martian meteorites reveals that apatite, amphibole, biotite, amorphous phases of melt inclusions, carbonate, impact-melt glasses, groundmass glasses, and even silicates have significantly higher δD (up to ~6,800‰) signatures than that of the Earth (Boctor et al., 2003; Giesting et al., 2015; Greenwood et al., 2008, 2010; Hallis et al., 2017; Hu et al., 2014, 2019; Hu, Lin, Zhang et al., 2020; Koike et al., 2016; Leshin, 2000; Leshin et al., 1996; Mane et al., 2016; Sugiura & Hoshino, 2000; Usui et al., 2012, 2015; Watson et al., 1994). However, some studies of Martian meteorites have indicated the presence of a D-poor reservoir on Mars (Gillet et al., 2002; Hallis et al., 2012a, 2012b; Leshin, 2000; Mane et al., 2016; Usui et al., 2012) by degassing from a mantle reservoir (Hu et al., 2019; Leshin, 2000). McCubbin and Barnes (2019) proposed that the Martian mantle retained some D-rich interstellar ice components, based on arguments developed using geochemical constraints on terrestrial planets, the Moon, and asteroids. Barnes et al. (2020) also proposed that the Martian mantle is chemically heterogeneous with multiple water reservoirs: The enriched mantle source has a D/H value of $(8.03 \pm 0.52) \times 10^{-4}$ and a water content of 36–72 ppm, the depleted mantle source has a D/H value of $>(1.99 \pm 0.02) \times 10^{-4}$ and a water content of 14–23 ppm, and the Martian crust has a D/H value of $(2.68–5.73) \times 10^{-4}$.

Chlorine has also been shown recently to have two significantly different isotopic reservoirs on Mars: a crustal/surficial reservoir enriched in ^{37}Cl relative to the Earth and a ^{37}Cl-depleted mantle reservoir (Sharp et al., 2016; Shearer et al., 2018; Williams et al., 2016). Martian meteorites have δ^{37}Cl values varying from ~ −4‰ to 8.6‰, supporting a two end-member mixing model (Sharp et al., 2016; Williams et al., 2016). The mantle reservoir was proposed to have a δ^{37}Cl of −4‰ to −3‰ (Sharp et al., 2016; Williams et al., 2016). The crustal/surficial reservoir has a δ^{37}Cl of ~2‰ (Sharp et al., 2016; Williams et al., 2016). This was suggested to have been caused by HCl loss from Mars' atmosphere, in a similar way to the loss of Martian water (Sharp et al., 2016; Williams et al., 2016). Heavier Cl isotopic compositions display a positive correlation with the Δ^{33}S (Williams et al., 2016). Such correlation is consistent with the binary model proposed by Sharp et al. (2016). Much lower δ^{37}Cl (down to -6.6 ± 0.8‰) has been reported by Shearer et al. (2018) in apatite from Chassigny. They proposed that the Martian mantle had a slightly lower δ^{37}Cl value (−4‰ to −6‰) compared to that suggested by Sharp et al. (2016).

In the study of Martian volatiles, apatite, $Ca_5(PO_4)_3$(F, Cl, OH), has received particular attention for constraining geological, biological, and hydrothermal processes in planetary environments (McCubbin & Jones, 2015). Hydrogen and Cl isotopic systematics in apatite have also advanced our understanding of geochemical processes on the Moon (e.g., Barnes et al., 2019; Boyce et al., 2015; Sharp et al., 2010; Tartèse et al., 2014), 4 Vesta (Barrett et al., 2019; Sarafian et al., 2017a), and in parent bodies of various achondrites (Sarafian et al., 2017b; Tartèse et al., 2019).

The first measurements of H isotopes in Martian apatite were reported by Watson et al. (1994). Since then, expanding H isotopic data sets of apatite in Martian meteorites have defined two distinct populations, one displaying a positive correlation (Guan et al., 2003; Hu et al., 2014) while the other displaying a negative correlation with water concentrations (Boctor et al., 2003; Greenwood et al., 2008; Hallis et al., 2012a; Hu et al., 2019; Koike et al., 2016; Leshin, 2000). Apatites in Martian meteorites are often highly fractured and small in size (< ~150 μm), with associated analytical challenges in avoiding any terrestrial contamination (e.g., weathering and/or epoxy) during their isotopic measurements. In the cases where water concentration is observed to display a negative correlation with δD, it has been interpreted in terms of dilution of a D-enriched Martian atmospheric component by variable levels of terrestrial contamination (Ross et al., 2011; Stephant et al., 2018) or by D-poor magmatic fluids on Mars (Hu et al., 2019; Leshin, 2000). In light of these previous studies, the H and Cl isotopic systematics of apatite in the Martian shergottite, NWA 8657, have been measured in situ to better understand the nature of volatiles in different Martian geochemical reservoirs. Apatite is an ideal target mineral of study because it hosts OH^- and Cl^- anions in its crystallographic structure. Previous petrologic work by Hu et al. (2016) and Howarth et al. (2018) identified abundant, large (up to ~200 μm in length), and smooth apatite grains, making NWA 8657 an ideal candidate for study. A NanoSIMS was used to investigate the H and Cl isotopic systematics of apatite. In addition, complementary data set in terms of concentrations of H_2O, F, S, and Cl of large and smooth apatite, merrillite, maskelynite, mesostasis, and pyroxene grains was also acquired. However, in this study, the variations in H and Cl

isotopic compositions of apatite are primarily used to discuss the evolution of different water reservoirs on Mars.

2. Materials and Methods

2.1. The Basaltic Shergottite NWA 8657

Northwest Africa (NWA) 8657 was found in 2014 and is probably paired with NWA 8656 (Irving et al., 2015). It has been classified as an enriched basaltic shergottite (Howarth et al., 2018). NWA 8657 was thought to have crystallized at 30–70 km depth followed by partial resorption en route to the surface. Subsequently, this rock experienced a strong impact event during which large melting zones were formed: redistributing REEs in shock melts (Howarth et al., 2018). A high-pressure polymorph of silica, coesite, has been reported in NWA 8657 (Hu, Li, et al., 2020). One polished chip of NWA 8657 was mounted in indium, following methods described in Hauri et al. (2002) and Hu et al. (2015), with a total surface area for examination at ~3 cm^2.

2.2. SEM and EPMA

Petrographic observations and X-ray elemental mapping were made using FEI Nova NanoSEM 450 field emission scanning electron microscope (FE-SEM) at the Institute of Geology and Geophysics, Chinese Academy of Sciences (IGGCAS), and a Zeiss SUPRA55 SEM at the National Astronomical Observatories, CAS. A JEOL JXA-8100 electron probe microanalyzer (EPMA) at IGGCAS was used for determining the major and minor elemental abundances in phosphates. The operating conditions included an accelerating voltage of 15 kV and a beam current of 20 nA with a defocused beam (spot diameter ~5 μm) for apatite measurements. The other analytical details for phosphate analysis are the same as those used by McCubbin et al. (2010). The EPMA standards used were jadeite (Na, Al, and Si), bustamite (Ca and Mn), pyrope (Mg), apatite (F, Cl, and P), hematite (Fe), K-feldspar (K), synthetic rutile (Ti), and Cr_2O_3 (Cr). Sodium, K, F, and Cl were measured first in order to minimize the loss of volatiles by electron beam irradiation. The detection limits are (1σ) 0.01 wt% for K_2O; 0.02 wt% for SiO_2, Cr_2O_3, Al_2O_3, MgO, CaO, Na_2O, P_2O_5, F, and Cl; 0.05 wt% for FeO; and 0.06 wt% for MnO. The Bence-Albee procedure was used for determining elemental abundances. The EPMA analytical results of apatite from NWA 8657 are listed in Repository Table 1 (Hu, Lin, Anand, et al., 2020).

2.3. Water Content and Hydrogen Isotopes

The hydrogen isotopes and water content of apatite, merrillite, maskelynite, mesostasis, and pyroxene from NWA 8657 were measured in situ with a Cameca NanoSIMS 50 L at the IGGCAS. The NWA 8657 polished chip and all the reference materials used in this work were mounted in indium. The sample and standards were installed in a sample holder and baked overnight at ~60°C in the NanoSIMS airlock. Then the sample holder was stored in the NanoSIMS sample chamber to improve the vacuum quality and minimize the H background (Hauri et al., 2002; Hu et al., 2014, 2015). Each 10 μm × 10 μm analysis areas were presputtered for ~2 min with a Cs^+ ion beam to remove surface coating and potential contaminations. The secondary anions of $^1H^-$, $^2D^-$, $^{12}C^-$, and $^{18}O^-$ were simultaneously counted by electron multipliers (EMs) from the central 5 μm × 5 μm areas using NanoSIMS blanking technique. The dead time (44 ns) of EMs was corrected, and the noise of EMs ($<10^{-2}$ cps) was ignored. The primary ion beam current was ~0.5 nA, and the beam size was ~500 nm in diameter. The charging effect on the sample surface was compensated by an electron-gun during analysis. San Carlos olivine was used for H background corrections following the relationship $H/O_{bg} = (H_{counts} - H_{bg})/O_{counts}$) and $D/H_{measured} = (1-f) \times D/H_{real} + f \times D/H_{bg}$, where f is the proportion of H from the instrument background (Hu, Lin, Zhang, et al., 2020; Tartèse et al., 2019), $D/H_{bg} = (2.30 \pm 0.75) \times 10^{-4}$ and $H_{bg} = (1.25 \pm 0.20) \times 10^5$ (2SD, $N = 8$, H_2O background is calculated to be 21 ± 11 ppm). The instrumental mass fractionation (IMF) and matrix effect on water content were established by measuring two apatite standards, Durango apatite (0.0478 wt% H_2O) (Greenwood et al., 2008, 2011) and Kovdor apatite (0.98 ± 0.07 wt% H_2O and $\delta D = -66 \pm 21‰$) (Nadeau et al., 1999). Hydrogen isotopic compositions are given in delta notation, $\delta D = ((D/H)_{sample}/(D/H)_{SMOW}) - 1) \times 1{,}000‰$, where SMOW is the standard mean ocean water with the D/H ratio of 1.5576×10^{-4}. More technical details can be found in Hu et al. (2014, 2015). All data are reported at 2σ uncertainties including reproducibility of D/H measurements on reference materials, uncertainty on H_2O background subtraction on San Carlos olivine, and internal precision on each analysis (Repository Table 2, Hu, Lin, Anand, et al., 2020).

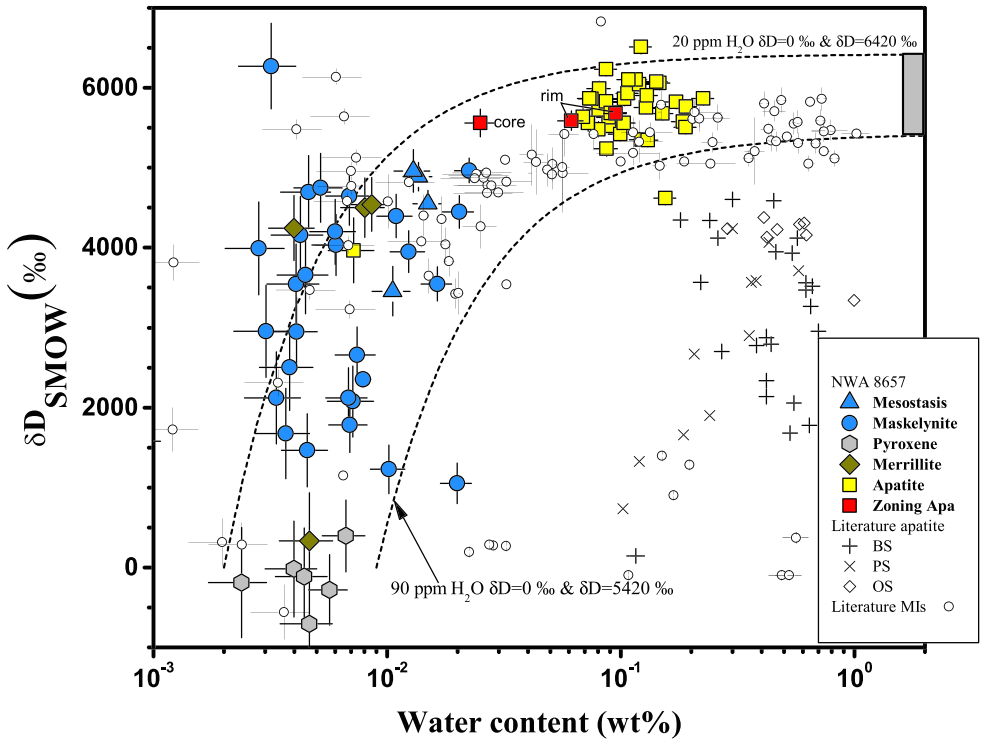

Figure 1. Water concentrations and associated δD values of apatite, merrillite, maskelynite, mesostasis, and pyroxene from NWA 8657. All analyses of the apatite, merrillite, maskelynite, mesostasis, and pyroxene plot within the mixing area between the initial water content of 20–90 ppm and δD of ~0‰ and the Martian crustal/surficial water (δD = 5,420–6,420‰, the shaded range on the right axis). Melt inclusion (MI) data are from Usui et al. (2012, 2015), Hu et al. (2014), Mane et al. (2016), Koike et al. (2016), Hallis et al. (2017), and Hu, Lin, Zhang, et al. (2020). Data for apatite: basaltic shergottites (BS) from Leshin (2000), Boctor et al. (2003), Greenwood et al. (2008), and Hallis et al. (2012a); poikilitic shergottites (PS) from Guan et al. (2003) and Hu et al. (2014); and olivine-phyric shergottites (OS) from Koike et al. (2016).

2.4. F, S, and Cl Contents and Chlorine Isotopes

Chlorine isotopes were measured in situ in apatite grains with a NanoSIMS 50 L at The Open University, using methods described in Barnes et al. (2016) and Tartèse et al. (2014). Each 7 μm × 7 μm analysis area was rastered with a Cs^+ beam using ~0.2 nA current for 2 min, eliminating any surface contamination. Secondary ionic species of $^{18}O^-$, $^{19}F^-$, $^{32}S^-$, $^{35}Cl^-$, $^{37}Cl^-$, and $^{40}Ca^{16}O^-$ were counted with EMs under multi-collection mode for 400 cycles using a 15 pA primary beam current from the central 5 μm × 5 μm areas. Three reference apatite grains AP004 (Cl = 4,100 ± 400 ppm, F = 2.39 ± 0.24 wt%, and S = 1,000 ± 120 ppm), AP005 (Cl = 9,500 ± 600 ppm, F = 2.45 ± 0.22 wt%, and S = 400 ± 120 ppm) and AP018 (Cl = 1,300 ± 400 ppm, F = 3.28 ± 0.38 wt%, and S = 3,640 ± 520 ppm) (McCubbin et al., 2012) were used to calibrate the F, S, and Cl concentrations for unknown samples. The calibration parameters are plotted in Figure S1. San Carlos olivine was used to calculate F, S, and Cl instrument background abundances of 6.8 ± 1.0, 0.5 ± 0.04, and 0.2 ± 0.01 ppm (2SD, n = 4), respectively, all of which are considered negligible relative to the measured abundances in the sample. As Cl contents of apatite from NWA 8657 are usually higher than 1.5 wt.%, AP005 (assumed identical to AP004 in chlorine isotopes) (Barnes et al., 2019) with the highest Cl content among available standards was used for applying instrumental mass fractionation correction. AP005 and apatite from NWA 8657 were internally analyzed in order to monitor the aging effect of the EM collectors. The reproducibility on AP005 across the entire analysis session is 1.2‰ (2SD, N = 10) (Figure S2). The chlorine isotopic composition is given in the form of $\delta^{37}Cl = (((^{37}Cl/^{35}Cl)_{sample}/(^{37}Cl/^{35}Cl)_{SMOC}-1) \times 1{,}000‰$, where SMOC is the standard mean ocean chloride with $^{37}Cl/^{35}Cl$ of 0.31977 and is reported with the associated 2σ uncertainties, which include the reproducibility of $^{37}Cl/^{35}Cl$ measurements on the reference apatite and internal uncertainty of each analysis (Repository Table 3, Hu, Lin, Anand, et al., 2020).

3. Results

The NWA 8657 polished section is mainly composed of pyroxene with patchy textures and plagioclase (transformed into maskelynite), with minor titanomagnetite, ilmenite, silica, mesostasis, and phosphates, with the typical texture of basaltic shergottite (Figure S3). The phosphates (~1.5 vol%) occur as intergrowths of apatite (1/3) and merrillite (2/3) (Figure S3). EPMA data for apatite confirm their F- and Cl-rich nature (Repository Table 1, Hu, Lin, Anand, et al., 2020; Figure S4). Apatite usually occurs in proximity of maskelynite, titanomagnetite, and ilmenite, with grain sizes up to ~200 μm in length and with a smooth appearance (Figure S5). Apatite rarely occurs near impact-melt pockets (Figures S5k and S5m).

The NanoSIMS analytical spots are shown in Figure S5. The water contents and δD values of the apatite, merrillite, maskelynite, mesostasis, and pyroxene are summarized in Repository Table 2 (Hu, Lin, Anand, et al., 2020). The apatite grains have relatively homogeneous and high δD values (~5,200–6,500‰) except for one chlorapatite grain (Figure S5k), which has a lower δD value of 3,965 ± 405‰ at relatively lower water content (72 ± 16 ppm). Zoning in an apatite grain was found in a shock-induced melt pocket with 250 ppm water content and a δD of 5,562‰ in the cores and up to 950 ppm water content and δD values of ~5,600‰ at the rims (Figure S5k and Repository Table 2, Hu, Lin, Anand, et al., 2020). Most apatite grains have relatively higher water contents (72–2,251 ppm) compared to other phases measured in this study. The apatite from NWA 8657 are characterized by some of the highest D-enrichment (3,965–6,509‰) observed among all other Martian meteorites (Boctor et al., 2003; Greenwood et al., 2008; Guan et al., 2003; Hu et al., 2014; Koike et al., 2016; Leshin, 2000; Watson et al., 1994). These δD values in apatite are comparable or even higher than the highest δD values reported for melt inclusions in basaltic shergottites (~6,040‰; Hu et al., 2014). In comparison, all analyses of merrillite are water poor (8–86 ppm) with associated δD values of 334–4,542‰. Maskelynite is also water poor (28–224 ppm) but with significant D-enrichment (δD up to ~6,200‰). Multiple analyses conducted along traverses on large grains of maskelynite reveal a water diffusion profile with higher H_2O contents (224 ppm) and δD values (4,965‰) at the rims and lower H_2O contents (45 ppm) and δD values (1,466‰) near the central areas (Repository Table 2, Hu, Lin, Anand, et al., 2020; Figure S6). All analyses of the water contents and δD values conducted on various phases plot along a two end-member mixing trend (Figure 1).

The Cl isotopic composition of apatite varies from −1.7 ± 1.4‰ to 4.0 ± 1.4‰ (Repository Table 3, Hu, Lin, Anand, et al., 2020), plotting in the range of most basaltic shergottites and nonshergottites reported by Sharp et al. (2016) and Williams et al. (2016). Chlorine, S, and F concentrations vary from ~1.3 to 6.2 wt.%, 133 to 1,494 ppm and 194 ppm to 2.42 wt.%, respectively (Repository Table 3, Hu, Lin, Anand, et al., 2020). Sulfur (133–1,496 ppm; Repository Table 3, Hu, Lin, Anand, et al., 2020) tenuously positively correlates with Cl, with 3 suggested distinct populations (Figure S7). A covariant diagram between $\delta^{37}Cl$ and δD of different apatite grains from NWA 8657 shows that these grains plot close to the end-member of Martian crustal/surficial water reservoir (Figure 3).

4. Discussions

4.1. Minimizing Terrestrial and Analytical Artifacts

Exposure of D-rich Martian phases to terrestrial environments could potentially lower their δD-values (Stephant et al., 2018). Fractured or uneven surfaces can also affect isotopic measurements in situ because they may contain terrestrial contamination or cause edge effects during NanoSIMS analysis. In the case of NWA 8657, the contribution from terrestrial alteration and microcracks was reduced by their large and smooth morphologies (Figure S5, Repository Table 2, Hu, Lin, Anand, et al., 2020). The potential contributions from the instrumental H_2O background during analysis have been subtracted and are typically less than 7% for apatites, except for the most Cl-rich apatite (f = 36%, where f is proportion of H_2O emitted from the analysis chamber) and a spot (f = 12%) in the center zone of the apatite found in the shock-induced melt (Repository Table 2, Hu, Lin, Anand, et al., 2020). The estimated instrumental H contribution on water content for merrillite, maskelynite, pyroxene, and mesostasis are ~45%, ~34%, ~41%, and ~17%, respectively, on average (Repository Table 2, Hu, Lin, Anand, et al., 2020), somewhat higher than that of apatite because of their low water concentrations. The water concentrations of NWA 8657 apatite, merrillite, maskelynite, mesostasis, and pyroxene all positively correlate with the δD values (Figure 1), suggesting virtually negligible

influence of terrestrial contamination; otherwise, a reverse trend in δD against H_2O would have been observed.

4.2. Formation of D-Rich Apatite

Apatite grains from NWA 8657 have higher δD values and mostly lower H_2O concentrations than those from other shergottites (Figure 1) and the data plot along a trend of increasing δD values versus H_2O concentration, as also identified in melt inclusions from GRV 020090 (Hu et al., 2014) and NWA 6162 (Hu, Lin, Zhang, et al., 2020). Such trends in apatite data have been reported only from studies of GRV 020090 (Hu et al., 2014) and GRV 99027 (Guan et al., 2003), suggesting progressive fractional crystallization from a magma, which assimilated D-enriched crustal/surficial water (Hu et al., 2014). Most apatite grains from other shergottites show H_2O to negatively correlate with δD except for a single spot from EETA 79001B with low H_2O and low δD (Boctor et al., 2003; Greenwood et al., 2008, 2010; Koike et al., 2016; Leshin, 2000). Such observations suggest either magmatic degassing on Mars (Hu et al., 2019; Leshin, 2000) or terrestrial contamination on Earth (Mane et al., 2016; Stephant et al., 2018). The positive correlation between H_2O and δD of apatite from NWA 8657 is significantly different from those in ALH 84001 (Boctor et al., 2003; Greenwood et al., 2008), the regolith breccia NWA 7034 and its pairs (Hu et al., 2019), nakhlites (Hallis et al., 2012a), and chassignites (Boctor et al., 2003), all of which display negative trends. This negative trend was probably due to the interaction between the degassing fluids from volcanic activities on Mars and the host rock (Boctor et al., 2003; Greenwood et al., 2008; Hallis et al., 2012a; Hu et al., 2019; Leshin, 2000). The positive correlation between H_2O and δD of NWA 8657 apatite, merrillite, mesostasis, maskelynite, and pyroxene (Figure 1) on the other hand is consistent with the mixing of D- and H_2O-poor and D- and H_2O-rich end-members (Hu et al., 2014; Hu, Lin, Zhang, et al., 2020; Liu et al., 2018). Since the δD value of the Martian mantle has been called into question (Leshin, 2000; Greenwood et al., 2008; Usui et al., 2012; Hallis et al., 2012a; Peslier et al., 2019; Barnes et al., 2020), two different models are discussed below to reconcile the data obtained in this study.

4.2.1. D-Poor Martian Mantle Model

It has been proposed that the D-rich apatite in Martian rocks formed either during crystallization of their parent melts that incorporated some D-rich water from Martian crustal material or during substantial but incomplete postcrystallization H exchange of apatite with D-enriched hydrous fluids on Mars (Watson et al., 1994). In the former case, similar D/H ratios would be expected for merrillite and apatite both of which formed at similar (late) crystallization stages (as also indicated by their textural relationship) at relatively high temperatures. However, the measured D/H ratios of merrillite are significantly lower than those of apatite (Figure 1). Furthermore, NWA 8657 is an extrusive rock with heavily shocked features (Howarth et al., 2018; Hu, Li, et al., 2020). The late crystallizing phases, for example, augite overgrowths and some plagioclase that formed after eruption, should have equilibrated with apatite in H isotopes because of the rapid diffusion rate of H at higher temperatures (Zhang & Behrens, 2000). However, large differences in D/H ratios were detected among pyroxene, maskelynite, merrillite, and apatite (Figure 1), which are inconsistent with high D/H ratios of apatite forming during the crystallization from its parental melt. Moreover, mesostasis from NWA 8657, the quenched materials from the residual melt, should have similar or even higher D/H ratios and higher water content (based on partitioning behavior of water between apatite and the residual melt). The mesostasis has significantly lower water content and D/H ratios than apatite except for the most Cl-rich apatite (Figure 1), which most likely formed later compared to the other apatites investigated in this study (Figure 1) based on the thermodynamic estimations and experiments (Boyce et al., 2014; McCubbin et al., 2015). If we assume that the Cl-rich apatite crystallized last and equilibrated with the residual melt, the estimated water content for the mesostasis could be 300–1,030 ppm when using the partition coefficient (0.07–0.24) of OH between apatite and melt determined by McCubbin et al. (2015). The measured water content of NWA 8657 mesostasis is however ~130 ppm, on average, significantly lower than the estimated value above. Alternatively, the Cl-rich apatite could have formed by the interaction of the magma with Cl-rich crustal fluids, but it is still difficult to explain the low water content of the mesostasis. Therefore, the significantly lower δD values of the residual melt (i.e., the mesostasis) and the merrillite might imply that the enhancement in δD values of apatite could possibly be attributed to selective fluid-mineral interactions during some postcrystallization event(s).

Other phases in NWA 8657 such as maskelynite/feldspathic glass display a range in δD values (1,051–6,272‰) and the water content (28–224 ppm) (Figure 1 and Repository Table 2, Hu, Lin, Anand,

et al., 2020), suggesting either a mixing between two distinct water reservoirs or progressive crystallization and assimilation by D-rich material. In the latter scenario, it is still difficult to explain the similarity in water content between plagioclase and mesostasis. Moreover, maskelynite displays a typical zoning profile in terms of the water contents and δD values decreasing from the rims toward the cores (Figure S6), similar to those of maskelynite from NWA 6162 (Hu, Lin, Zhang, et al., 2020), melt inclusions from GRV 020090 (Hu et al., 2014), and impact-melt glasses from Tissint (Chen et al., 2015), consistent with inward diffusion of Martian surficial D-rich water after/during the transformation of plagioclase to maskelynite (Figure S6). Liu et al. (2018) modeled D-rich water diffusion by shock to explain the high δD and water content of maskelynite adjacent to a shock melt vein in EETA 79001. The zoned maskelynite measured in this work is however far (>1,000 μm) away from any shock-melt phases (Figure S5e). In the highly shocked Tissint (e.g., Aoudjehane et al., 2012), most maskelynite have low δD values, while impact-melt glasses are D- and volatile-enriched (Chen et al., 2015), indicating that hydrogen isotopes in most maskelynite were not strongly affected by the shock-induced metamorphism. Meanwhile, some apatite grains, for example, zoned apatite grain #30 in a shock-melt pocket (Figure S5m), also have higher water contents at the rims but with homogeneous high D/H ratios across the grain (Repository Table 2, Hu, Lin, Anand, et al., 2020; Figure 1). These characteristics favor a preferential (postshock) addition of D-rich water in apatite (Figure 1). Any interaction with terrestrial waters should have diluted the D-enrichments at the rims, which has not been observed here (see section 4.1). Degassing of the parent magma also cannot account for the large fractionation of H isotopes in NWA 8657 apatite (Repository Table 2, Hu, Lin, Anand, et al., 2020; Figure 1), because water typically fractionates less than 500‰ (Sharp et al., 2013) under the Log fO_2 (FMQ) ~ 0 oxygen fugacity (Howarth et al., 2018). If NWA 8657 apatite interacted with a D-rich fluid by dissolution and reprecipitation (Kusebauch et al., 2015), the igneous textures of apatite should not have been preserved (Figure S5). It is difficult to explain how magmatic apatite could have retained a D-rich isotope signature without some form of interaction with crustal fluids on the surface of Mars.

4.2.2. D-Rich Martian Mantle Model

Recently, Barnes et al. (2020) have proposed that the enriched mantle, the depleted mantle, Martian crust, and Martian atmosphere have δD values of 4,155 ± 333‰, >264 ± 13‰, 721–2,679‰, and 4,001–5,478‰, respectively. NWA 8657 is an enriched basaltic shergottite (Howarth et al., 2018). Given the enriched mantle source of Mars having a δD of 4,155 ± 333‰ as proposed by Barnes et al. (2020), one would expect to find high-δD signatures in primary pyroxene and plagioclase. However, the pyroxene in NWA 8657 has a water content of 46 ppm (approximately two times higher than instrumental H_2O background) with an associated average δD of −151‰ (Repository Table 2, Hu, Lin, Anand, et al., 2020), which, incidentally, is consistent with the Martian mantle having a terrestrial like hydrogen isotopic signature argued for by previous workers (Hallis et al., 2012a; Usui et al., 2012). The low δD values of pyroxene from NWA 8657 argue against the potential degassing effects during/before crystallization of pyroxene (Peslier et al., 2019). Another potential effect to consider is shock metamorphism. In the case of EETA 79001C, Liu et al. (2018) found that the hydrogen isotopic compositions of pyroxene is easier to reset than olivine by shock because of their difference in water capacity. Although NWA 8657 contains rare but highly shocked olivine grains (Howarth et al., 2018; Hu, Li, et al., 2020), no D-rich signature is observed, indicating that the shock metamorphism did not affect the H isotope systematics of silicate phases in NWA 8657 (Figure 1). Thus, the positive relationship between the water content and the δD values of pyroxene, maskelynite, mesostasis, and apatite from NWA 8657 (Figure 1) is compatible with the Martian mantle having a terrestrial like D/H ratio and the D-rich signatures of apatite were most likely a result of postshock surface water-rock interaction on Mars. Hereafter, the D-poor Martian mantle model will be used in further discussions below.

4.3. Formation of ^{37}Cl-Rich Apatite

The surface reservoir of volatiles on Mars is not only D-rich but also rich in other stable isotopes (e.g., ^{34}S and ^{13}C) (Franz et al., 2014; Webster et al., 2013) compared to its mantle. The δ^{37}Cl value of the crustal/surficial reservoir was reported to be ~2‰ by Sharp et al. (2016) based on the bulk analysis of several Martian meteorites. However, a measurement on an apatite grain from NWA 7034 (Sharp et al., 2016; Williams et al., 2016) was made at ~8‰, necessitating further research for constraining the range of δ^{37}Cl in Martian materials. The bulk-rock δ^{37}Cl values of most Martian meteorites positively correlate with Δ^{33}S (Williams et al., 2016). Positive Δ^{33}S values are an indicator of UV-related photochemical reactions that took place at higher altitudes of the atmosphere (Franz et al., 2014). This is also consistent with isotopic exchange between the

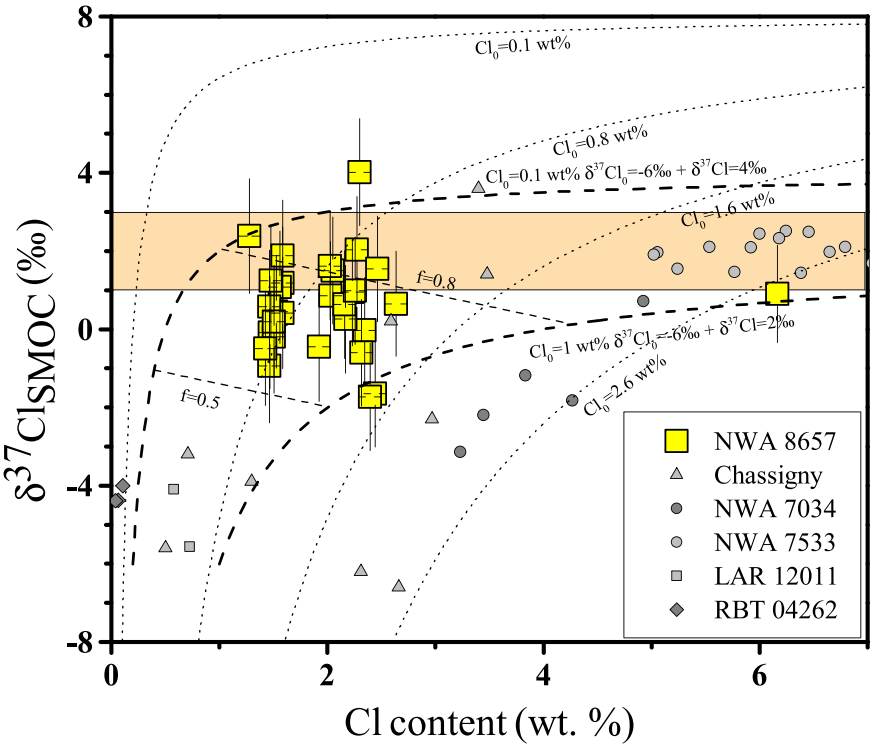

Figure 2. The chlorine concentrations and the δ^{37}Cl values of apatite from NWA 8657. Apatite grains from NWA 8657 are mainly distributed in or close to the range of the Martian crustual/surficial reservoir ($\delta^{37}Cl = 2 \pm 1‰$; Sharp et al., 2016; hatched area). Dashed lines represent the mixing trend of two end-members, one end-member is the heavy-Cl crustal/surficial reservoir with δ^{37}Cl of 2‰ to 4‰ proposed by Sharp et al. (2016), and the other end-member is the light-Cl mantle reservoir with primordial Cl concentrations (Cl_0) of 0.1–1.0 wt.% and $\delta^{37}Cl_0$ of −6‰ (Shearer et al., 2018). Fractions (f) of crustal/surficial reservoir recorded in apatite from NWA 8657 vary from 0.5 to 0.8 or slightly higher. Dotted lines represent the mixing trend of two end-members with different initial values, Cl_0 = 0.1–2.6 wt% and $\delta^{37}Cl_0$ of −8‰ (slightly lower than the minimum value reported by Shearer et al., 2018) for mantle reservoir and δ^{37}Cl of + ~8‰ (highest value reported in Williams et al., 2016, and Sharp et al., 2016) for crustal/surficial reservoir. Literatures data for apatite: Chassigny from Shearer et al. (2018), NWA 7533, LAR 12011, and RBT 04262 from Bellucci et al. (2017) excluding the low F- and Cl-spots, NWA 7034 from Hu et al. (2019).

atmosphere and the surface reservoir. Thus, Martian meteorites potentially record the chlorine isotopic compositions of different reservoirs on Mars (Bellucci et al., 2017; Sharp et al., 2016; Shearer et al., 2018; Williams et al., 2016); the highest δ^{37}Cl value from Martian meteorites is thought to be from the crustal/surficial heavy-Cl reservoir (Bellucci et al., 2017; Hu et al., 2019; Sharp et al., 2016; Williams et al., 2016), and the lowest δ^{37}Cl value is taken as representative of the light-Cl mantle reservoir (Shearer et al., 2018).

The chlorine isotopic compositions of NWA 8657 apatite mostly plot close to the ranges of the Martian crustal/surficial reservoir (Sharp et al., 2016; Williams et al., 2016) (Figures 2 and 3). This is significantly different compared to the Chassigny data (Boctor et al., 2003; Shearer et al., 2018). NWA 8657 apatite may have therefore also equilibrated with a ^{37}Cl-rich crustal/surface reservoir via ^{37}Cl-rich fluids. Martian magmatic systems have been explored to account for the presence of Cl-amphibole (Sautter et al., 2006); scapolite (Filiberto et al., 2014) in Nakhla; jarosite and hematite in a pyroxene-hosted melt inclusion in MIL 03346 (McCubbin et al., 2009); systematic chemical variations of apatite in Chassigny (McCubbin & Nekvasil, 2008); and variable Cl and high OH contents of apatite in LAR 06319 and LAR 12011 (Howarth et al., 2016). In these cases, magmatic hydrothermal fluids have been modeled in a low δD and a low δ^{37}Cl system (Hallis et al., 2012a; Sharp et al., 2016; Shearer et al., 2018; Usui et al., 2012; Williams et al., 2016). Apatite in NWA 8657 is clearly different; it is D- and ^{37}Cl-rich. This suggests involvement of a distinct surficial process. Possibilities include a hydrothermal source (e.g., melting of permafrost or the

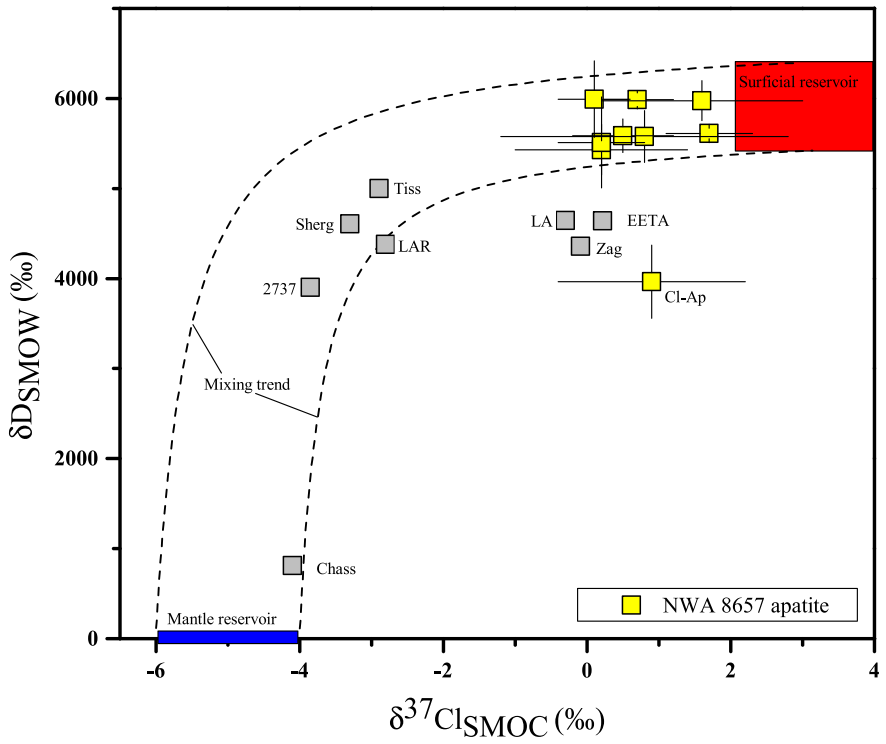

Figure 3. Plot of spatially related $\delta^{37}Cl$ and δD values for individual apatite grains from NWA 8657. Data sets are referred to the average values of different apatite grains in Repository Tables 2 and 3 (Hu, Lin, Anand, et al., 2020). Most apatite grains from NWA 8657 plot close to the Martian crustal/surficial water and Cl reservoir except for the chlorapatite with lower δD. The upper dashed line represents mixing of two end-members—$\delta^{37}Cl = -6‰$ (Shearer et al., 2018) and δD = 0‰ (Hallis, Taylor, Nagashima, Huss, Needham, et al., 2012)—with the Martian crustal/surficial reservoir—$\delta^{37}Cl = 4‰$ (Sharp et al., 2016; Williams et al., 2016) and δD = ~6,400‰ (maximum value measured in this work). The lower dashed line represents mixing of an end-member with $\delta^{37}Cl = -4‰$ (Sharp et al., 2016; Williams et al., 2016) and δD = 0‰ (Hallis et al., 2012a) with the Martian crustal/surficial reservoir with $\delta^{37}Cl = 4‰$ (Sharp et al., 2016; Williams et al., 2016) and δD = ~5,400‰ (estimated from Figure 1), assuming $H_2O_0 = 55$ ppm (estimated from Figure 1), $Cl_0 = 0.6$ wt% (estimated from Figure 2 for most apatite grains), $H_2O_{crustal} = 5$ wt% and $H_2O/Cl_{crustal} = 1$, where subscript 0 represents initial state of apatite prior to mixing by the suggested crustal/surficial end-member. Shaded region on top right: Martian surfacial/crustal reservoir. Shaded region on bottom left: mantle reservoir. $\delta^{37}Cl$ values of Chassigny (apatite in melt inclusions) from Shearer et al. (2018) and the other data sets from Williams et al. (2016) and Sharp et al. (2016). δD values plotted here are the highest values reported so far. Chassigny (Chass) from Boctor et al. (2003), NWA 2737 (2737) from Giesting et al. (2015), Shergotty (Sherg) from Greenwood et al. (2008), LAR 06319 (LAR) from Koike et al. (2016), Tissint (Tiss) from Lin et al. (2019), Zagami (Zag) from Watson et al. (1994), EETA 79001C (EETA) from Liu et al. (2018), and Los Angeles (LA) from Greenwood et al. (2010).

dissolution of Cl-salts in sediments) or a direct exchange between atmosphere and surface of Mars. If NWA 8657 reacted with a D- and ^{37}Cl-rich hydrothermal fluid, it would have been via diffusional exchange. The various δD values measured in apatite, merrillite, mesostasis, maskelynite, and pyroxene (Figure 1) would thus be a function of diffusional velocities of H and Cl in these phases (see in section 4.5.1). This could account for the zoning profiles observed in maskelynite, with δD values and water contents decreasing from the margins toward the central areas (Figure S6).

4.4. Relationship Between S and Cl Content of Apatite

The sulfur content of NWA 8657 apatite is similar to that of apatite from basaltic shergottites and terrestrial samples but significantly higher than those of other types of Martian meteorites except for Dhofar 019 (Channon, 2013; McCubbin et al., 2012, 2016). However, the positive correlation between S and Cl is distinctive compared to the other basaltic shergottites (Figure S7), indicating that some S in these apatite grains could be present as $S^{6+} + S^{4+}$ substituting $2P^{5+}$ (Kim et al., 2017; Konecke et al., 2017, 2019) under relatively high oxygen fugacity conditions (Channon, 2013; Howarth et al., 2018), probably during the latest

crystallization stage or during the later water-rock interaction event as discussed above. Although more detailed work may be required to clarify the formation mechanism, the oxygen isotopic compositions of phosphates from some other shergottites reported by Bellucci et al. (2020) favor the surface water-rock interaction scenario. The S contents of apatite from NWA 8657 are significantly higher than that of lunar apatite (Figure S7; Boyce et al., 2010), in which S is dominated by S^{2-} substitution at X site of apatite confirmed by the X-ray Absorption Near Edge Structure (XANES) analysis (Brounce et al., 2019). This is consistent with the difference in oxygen fugacity between Martian and lunar magmatic systems (Brounce et al., 2019; Howarth et al., 2018).

4.5. Implications

4.5.1. Rapid Equilibration of H Isotopes in Martian Apatite

Apatite is a hydrous mineral prone to chemical exchange with external fluids at relatively low temperatures as indicated by thermodynamic modeling (Zhu & Sverjensky, 1991) and synthetic experiments (Kusebauch et al., 2015). As depicted before, the positive correlation between the water contents and δD values of apatite, merrillite, maskelynite, and mesostasis suggests a two end-member mixing trend (Figure 1), one end-member is probably the Martian surficial water reservoir with δD of ~5,400 to ~6,400‰, and the other end-member is water hosted in the relatively higher-temperature mineral constituents of the rock with water concentrations varying from 20 to 90 ppm and δD of ~0‰. This would suggest that apatite, merrillite, maskelynite, and mesostasis would have similar water concentrations (20–90 ppm) prior to their interactions with the Martian surficial water. Such similarities could relate to a common petrogenesis, for example, dynamic formation mechanism of apatite (Boyce et al., 2014; McCubbin et al., 2015), magma degassing (Howarth et al., 2018), and shock metamorphism (Hu, Li, et al., 2020), because apatite typically has a higher water content than merrillite and maskelynite. It is not clear whether the low water content and low δD end-member are a magmatic signature or the result of later geologic events. We assume this end-member as a starting point before hydrothermal activity began, in order for estimating the contribution of the hydrothermal fluid.

The exceptional D-enrichment of apatite in NWA 8657 relative to the other shergottites suggests that the water retained in the apatite was mostly sourced from the surficial water reservoir. Accordingly, the mass fraction of surface water in the apatite can be calculated in terms of the mass balance following a similar approach described in Hu, Lin, Zhang, et al. (2020). The mass fractions (F in Repository Table 2, Hu, Lin, Anand, et al., 2020) of the Martian surface water retained in apatite, merrillite, mesostasis, maskelynite, and pyroxene from NWA 8657 are 80–99% with one exception (~60%) of the lowest water content of 72 ppm, 2–69%, 56–78%, 17–69%, and <8% respectively, when assuming the initial water content is the intermediate value (55 ppm) of the mixing trend lines. It indicates that all apatite grains from NWA 8657 have highly exchanged with the Martian crustal/surficial water reservoir.

D-rich features of Martian apatite grains have been known for several decades (Watson et al., 1994). The H isotopic compositions of NWA 8657 apatite, up to 6,509‰, are similar to those in GRV 020090 (Hu et al., 2014) and NWA 6162 melt inclusions (Hu, Lin, Zhang, et al., 2020), suggesting that both apatite and glassy phases of melt inclusions in Martian meteorites were reset in H isotopic compositions by surficial water interactions on Mars. Although the exchange coefficients of fluid with minerals/phases are temperature and time dependent (e.g., Friedman et al., 1966), the mass contribution from the D-rich water from Mars's surface could be used to estimate the relative exchange coefficients. The apatites in NWA 8657 and melt inclusion glasses in GRV 020090 (Hu et al., 2014) and NWA 6162 (Hu, Lin, Zhang, et al., 2020) have obvious high δD values (Figure 1), suggesting that they are highly equilibrated with the D-rich water reservoir on Mars and that the exchange coefficients of fluid with glassy phases and apatite may have comparable values. However, most apatite grains from basaltic shergottites have lower δD values, which negatively correlate with the water contents (Figure 1). One explanation could be contamination by D-poor water in NWA or during sample preparation and analysis (Mane et al., 2016; Stephant et al., 2018). There could also have been D-poor water rock interaction on Mars (Hu et al., 2019; Leshin, 2000). The negative correlation between water content and δD complicates the origin of the D-poor water. However, coordinating H and Cl isotopic systematics for additional Martian apatite grains would contribute greatly in clarifying this issue.

The high δD signatures of apatite indicate almost complete alteration by surficial D-rich Martian water. In the case of apatite from NWA 8657, which contained only 55 ± 35 ppm initial water (Figure 1), minute

addition of D-rich water would have strongly raised the δD values. In addition, the ease with which apatite alters its OH^-, Cl^-, and F^- with external fluids at relatively low temperatures (Kusebauch et al., 2015; Zhu & Sverjensky, 1991) would have further elevated its water content up to 2,287 ppm during alteration (Repository Table 2, Hu, Lin, Anand, et al., 2020). The D-rich water diffusional profiles in NWA 8657 maskelynite (Figure S6) is similar to the profiles in impact melt glasses from Tissint (Chen et al., 2015) but is clearly lower than that measured in the GRV 020090 glassy phases in melt inclusions (Hu et al., 2014) as well as NWA 8657 apatite (Figure 1). Although the water diffusion/exchange coefficients in maskelynite and mafic impact melt glasses under low temperature have not been measured yet, it is likely that the water diffusion/exchange coefficients are $D_{apatite/fluid}$ (probably comparable to $D_{MI/fluid}$) > $D_{mesostasis/fluid}$ ≈ $D_{maskelynite/fluid}$ ≈ $D_{merrllite/fluid}$ > $D_{pyroxene/fluid}$ on the basis of the measured water content of these phases along the positive trend in Figure 1. Diffusivities of H between fluids and apatite and silicates should be measured in future to further evaluate this possibility.

4.5.2. Martian Apatite Recording Late Hydrothermal Events on Mars

Apatite was once widely used to estimate the water content of the parent magma ~10 years ago (Boyce et al., 2010; McCubbin et al., 2012). More recently, it was found that the F^-, Cl^-, and OH^- concentrations of apatite are dependent on the compositions of the parent magma and crystallization sequences (Boyce et al., 2014; McCubbin et al., 2015). In addition, the isotopic compositions of apatites also tend to exchange rapidly with external fluids after crystallization as observed by large variations in δD (Boctor et al., 2003; Greenwood et al., 2008; Guan et al., 2003; Hu et al., 2014; Hu, Lin, Zhang, et al., 2020; Koike et al., 2016; Leshin, 2000) and $\delta^{37}Cl$ values (Bellucci et al., 2017; Hu et al., 2019; Sharp et al., 2016; Shearer et al., 2018; Williams et al., 2016) in many Martian meteorites. It means that most Martian apatite grains are not pristine if they are D- and ^{37}Cl-rich. Moreover, in such cases, Cl concentrations of the Martian mantle reservoir might have been overestimated based on apatite or bulk-rock analysis (Filiberto et al., 2016, 2016; Filiberto & Treiman, 2009).

Amphibole and biotite, another two OH- and Cl-bearing phases found in melt inclusions in some Martian meteorites, have significantly higher δD values (Giesting et al., 2015; Watson et al., 1994) than the Martian mantle at ~0‰ (Hallis et al., 2012a; Mane et al., 2016; Usui et al., 2012). Initially, all phases in melt inclusions should equilibrate with the Martian mantle during crystallization. However, the measured δD values of amphibole and biotite from Martian meteorites (Giesting et al., 2015; Watson et al., 1994) are significantly higher than expected. Furthermore, some apatite grains in the melt inclusions from Martian meteorites also have high δD values (Boctor et al., 2003). These features suggest that most hydrous minerals/phases from Martian meteorites exchanged with the crustal/surficial water reservoir, if the Martian mantle was D-poor.

5. Conclusions

Apatite from NWA 8657 has the highest δD value (up to 6,509‰) of any phosphates in Martian meteorites that is similar to the values of the modern Martian atmosphere. The δD values of apatite, merrillite, mesostasis, maskelynite, and pyroxene from NWA 8657 positively correlate with the water concentrations, suggesting interactions between Martian water and the parent rock of NWA 8657. Chlorine in NWA 8657 apatite exchanged with the external fluids as well as D, although in a smaller proportions compared to that of water. Both H and Cl isotopic compositions of apatite fit within a two end-member mixing model with a heavier isotope-enriched crustal/surficial reservoir at one end and a lighter isotope-enriched mantle reservoir at the other. The Martian crustal/surface reservoir seems to have a $\delta^{37}Cl$ value of approximately 2‰ to 4‰, consistent with the value measured in bulk Martian samples. Martian apatite water and Cl content, combined with H and Cl isotopic systematics, provide constrains on the compositions of volatiles in fluids on the surface of Mars and the potential geochemical reservoirs they are sourced from. The new data sets of H and Cl isotopic compositions from NWA 8657 favors a terrestrial like D/H ratio for the Martian mantle while the surface reservoir(s) of volatiles on Mars is not only D-enriched but also ^{37}Cl-enriched.

Conflict of Interest

The authors declare no competing financial interests.

Data Availability Statement

All data related to this work can be found in Hu, Lin, Anand, et al. (2020).

Acknowledgments

We thank David Chew and Fuyuan Wu for providing Kovdor and Durango apatites, editor Dr. Deanne Rogers and AE Dr. Mariek Schmidt for handling the manuscript, and three anonymous referees' suggestions and comments for improving the quality of the manuscript. This study was financially supported by the National Natural Science Foundation of China (41973062, 41573057, 41430105, and 41490631), China Scholarship Council (201804910284), the UK STFC grant to MA and IAF (#ST/P000657/1), and the key research program of the Institute of Geology & Geophysics, CAS (IGGCAS-201905).

References

Aoudjehane, H. C., Avice, G., Barrat, J. A., Boudouma, O., Chen, G., Duke, M. J. M., et al. (2012). Tissint Martian meteorite: A fresh look at the interior, surface, and atmosphere of Mars. *Science*, *338*(6108), 785–788. https://doi.org/10.1126/science.1224514

Barnes, J. J., Franchi, I. A., McCubbin, F. M., & Anand, M. (2019). Multiple reservoirs of volatiles in the Moon revealed by the isotopic composition of chlorine in lunar basalts. *Geochimica et Cosmochimica Acta*, *266*, 144–162. https://doi.org/10.1016/j.gca.2018.12.032

Barnes, J. J., McCubbin, F. M., Santos, A. R., Day, J. M. D., Boyce, J. W., Schwenzer, S. P., et al. (2020). Multiple early-formed water reservoirs in the interior of Mars. *Nature Geoscience*, *13*(4), 260–264. https://doi.org/10.1038/s41561-020-0552-y

Barnes, J. J., Tartèse, R., Anand, M., McCubbin, F. M., Neal, C. R., & Franchi, I. A. (2016). Early degassing of lunar urKREEP by crust-breaching impact(s). *Earth and Planetary Science Letters*, *447*, 84–94. https://doi.org/10.1016/j.epsl.2016.04.036

Barrett, T. J., Barnes, J. J., Anand, M., Franchi, I. A., Greenwood, R. C., Charlier, B. L. A., et al. (2019). Investigating magmatic processes in the early solar system using the Cl isotopic systematics of eucrites. *Geochimica et Cosmochimica Acta*, *266*, 582–597. https://doi.org/10.1016/j.gca.2019.06.024

Bellucci, J. J., Whitehouse, M. J., John, T., Nemchin, A. A., Snape, J. F., Bland, P. A., & Benedix, G. K. (2017). Halogen and Cl isotopic systematics in Martian phosphates: Implications for the Cl cycle and surface halogen reservoirs on Mars. *Earth and Planetary Science Letters*, *458*, 192–202. https://doi.org/10.1016/j.epsl.2016.10.028

Bellucci, J. J., Whitehouse, M. J., Nemchin, A. A., Snape, J. F., Kenny, G. G., Merle, R. E., et al. (2020). Tracing Martian surface interactions with the triple O isotope compositions of meteoritic phosphates. *Earth and Planetary Science Letters*, *531*, 115977. https://doi.org/10.1016/j.epsl.2019.115977

Boctor, N. Z., Alexander, C. M. O., Wang, J., & Hauri, E. (2003). The sources of water in Martian meteorites: Clues from hydrogen isotopes. *Geochimica et Cosmochimica Acta*, *67*(20), 3971–3989. https://doi.org/10.1016/S0016-7037(03)00234-5

Boyce, J. W., Liu, Y., Rossman, G. R., Guan, Y., Eiler, J. M., Stolper, E. M., & Taylor, L. A. (2010). Lunar apatite with terrestrial volatile abundances. *Nature*, *466*(7305), 466–469. https://doi.org/10.1038/nature09274

Boyce, J. W., Tomlinson, S. M., McCubbin, F. M., Greenwood, J. P., & Treiman, A. H. (2014). The lunar apatite paradox. *Science*, *344*(6182), 400–402. https://doi.org/10.1126/science.1250398

Boyce, J. W., Treiman, A. H., Guan, Y., Ma, C., Eiler, J. M., Gross, J., et al. (2015). The chlorine isotope fingerprint of the lunar magma ocean. *Science Advances*, *1*(8), e1500380. https://doi.org/10.1126/sciadv.1500380

Brounce, M., Boyce, J., McCubbin, F. M., Humphreys, J., Reppart, J., Stolper, E., & Eiler, J. (2019). The oxidation state of sulfur in lunar apatite. *American Mineralogist*, *104*(2), 307–312. https://doi.org/10.2138/am-2019-6804

Carr, M. H. (1987). Water on Mars. *Nature*, *326*(6108), 30–35. https://doi.org/10.1038/326030a0

Channon, M. B. (2013). *Oxygen isotopes and volatiles in Martian meteorite* (PhD Thesis). Pasadena, CA: California Institute of Technology.

Chen, Y., Liu, Y., Guan, Y., Eiler, J. M., Ma, C., Rossman, G. R., & Taylor, L. A. (2015). Evidence in Tissint for recent subsurface water on Mars. *Earth and Planetary Science Letters*, *425*, 55–63. https://doi.org/10.1016/j.epsl.2015.05.004

Ehlmann, B. L., Mustard, J. F., Murchie, S. L., Bibring, J. P., Meunier, A., Fraeman, A. A., & Langevin, Y. (2011). Subsurface water and clay mineral formation during the early history of Mars. *Nature*, *479*(7371), 53–60. https://doi.org/10.1038/nature10582

Elkins-Tanton, L. T., Hess, P. C., & Parmentier, E. M. (2005). Possible formation of ancient crust on Mars through magma ocean processes. *Journal of Geophysical Research*, *110*, E12S01. https://doi.org/10.1029/2005JE002480

Filiberto, J., Baratoux, D., Beaty, D., Breuer, D., Farcy, B. J., Grott, M., et al. (2016). A review of volatiles in the Martian interior. *Meteoritics & Planetary Science*, *51*(11), 1935–1958. https://doi.org/10.1111/maps.12680

Filiberto, J., Gross, J., & McCubbin, F. M. (2016). Constraints on the water, chlorine, and fluorine content of the Martian mantle. *Meteoritics & Planetary Science*, *51*(11), 2023–2035. https://doi.org/10.1111/maps.12624

Filiberto, J., & Treiman, A. H. (2009). Martian magmas contained abundant chlorine, but little water. *Geology*, *37*(12), 1087–1090. https://doi.org/10.1130/G30488A.1

Filiberto, J., Treiman, A. H., Giesting, P. A., Goodrich, C. A., & Gross, J. (2014). High-temperature chlorine-rich fluid in the Martian crust: A precursor to habitability. *Earth and Planetary Science Letters*, *401*, 110–115. https://doi.org/10.1016/j.epsl.2014.06.003

Franz, H. B., Kim, S. T., Farquhar, J., Day, J. M., Economos, R. C., McKeegan, K. D., et al. (2014). Isotopic links between atmospheric chemistry and the deep sulphur cycle on Mars. *Nature*, *508*(7496), 364–368. https://doi.org/10.1038/nature13175

Friedman, I., Smith, R. L., & Long, W. D. (1966). Hydration of natural glass and formation of perlite. *Geological Society of America Bulletin*, *77*(3), 323–328. https://doi.org/10.1130/0016-7606(1966)77[323:Hongaf]2.0.Co;2

Giesting, P. A., Schwenzer, S. P., Filiberto, J., Starkey, N. A., Franchi, I. A., Treiman, A. H., et al. (2015). Igneous and shock processes affecting chassignite amphibole evaluated using chlorine/water partitioning and hydrogen isotopes. *Meteoritics & Planetary Science*, *50*(3), 433–460. https://doi.org/10.1111/maps.12430

Gillet, P., Barrat, J. A., Deloule, E., Wadhwa, M., Jambon, A., Sautter, V., et al. (2002). Aqueous alteration in the Northwest Africa 817 (NWA 817) Martian meteorite. *Earth and Planetary Science Letters*, *203*(1), 431–444. https://doi.org/10.1016/S0012-821X(02)00835-X

Greenwood, J. P., Itoh, S., Sakamoto, N., Vicenzi, E. P., & Yurimoto, H. (2008). Hydrogen isotope evidence for loss of water from Mars through time. *Geophysical Research Letters*, *35*, L05203. https://doi.org/10.1029/2007GL032721

Greenwood, J. P., Itoh, S., Sakamoto, N., Vicenzi, E. P., & Yurimoto, H. (2010). D/H zoning in apatite of Martian meteorites QUE 94201 and Los Angles: Implications for water on Mars In *Paper presented at 73rd annual meeting of the meteoritical society, July* (Vol. 45, p. A68). New York, NY, USA: The meteoretical society.

Greenwood, J. P., Itoh, S., Sakamoto, N., Warren, P., Taylor, L., & Yurimoto, H. (2011). Hydrogen isotope ratios in lunar rocks indicate delivery of cometary water to the Moon. *Nature Geoscience*, *4*(2), 79–82. https://doi.org/10.1038/ngeo1050

Guan, Y., Hsu, W., Leshin, L. A., Wang, H., Wang, R., Zhang, F., et al. (2003). Hydrogen isotopes of phosphates in the New Martian Meteorite GRV 99027. In *Paper presented at 34th Lunar and Planetary Science Conference, March* (Vol. 34, p. 1830). Houston, USA: Lunar and Planetary Institute.

Hallis, L. J. (2017). D/H ratios of the inner solar system. *Philosophical Transactions. Series A, Mathematical, Physical, and Engineering Sciences*, *375*(2094), 20150390. https://doi.org/10.1098/rsta.2015.0390

Hallis, L. J., Huss, G. R., Nagashima, K., Taylor, G. J., Stöffler, D., Smith, C. L., & Lee, M. R. (2017). Effects of shock and Martian alteration on Tissint hydrogen isotope ratios and water content. *Geochimica et Cosmochimica Acta*, *200*, 280–294. https://doi.org/10.1016/j.gca.2016.12.035

Hallis, L. J., Taylor, G. J., Nagashima, K., & Huss, G. R. (2012a). Magmatic water in the Martian meteorite Nakhla. *Earth and Planetary Science Letters*, *359-360*, 84–92. https://doi.org/10.1016/j.epsl.2012.09.049

Hallis, L. J., Taylor, G. J., Nagashima, K., Huss, G. R., Needham, A. W., Grady, M. M., & Franchi, I. A. (2012b). Hydrogen isotope analyses of alteration phases in the nakhlite Martian meteorites. *Geochimica et Cosmochimica Acta*, *97*, 105–119. https://doi.org/10.1016/j.gca.2012.08.017

Hauri, E., Wang, J., Dixon, J. E., King, P. L., Mandeville, C., & Newman, S. (2002). SIMS analysis of volatiles in silicate glasses: 1. Calibration, matrix effects and comparisons with FTIR. *Chemical Geology*, *183*(1–4), 99–114. https://doi.org/10.1016/S0009-2541(01)00375-8

Howarth, G. H., Liu, Y., Chen, Y., Pernet-Fisher, J. F., & Taylor, L. A. (2016). Postcrystallization metasomatism in shergottites: Evidence from the paired meteorites LAR 06319 and LAR 12011. *Meteoritics & Planetary Science*, *51*(11), 2061–2072. https://doi.org/10.1111/maps.12576

Howarth, G. H., Udry, A., & Day, J. M. D. (2018). Petrogenesis of basaltic shergottite Northwest Africa 8657: Implications for fO_2 correlations and element redistribution during shock melting in shergottites. *Meteoritics & Planetary Science*, *53*(2), 249–267. https://doi.org/10.1111/maps.12999

Hu, S., Li, Y., Gu, L., Tang, X., Zhang, T., Yamaguchi, A., et al. (2020). Discovery of coesite from the Martian shergottite Northwest Africa 8657. *Geochimica et Cosmochimica Acta*, *286*, 404–417. https://doi.org/10.1016/j.gca.2020.07.021

Hu, S., Lin, Y., Anand, M., Franchi, I. A., Zhao, X., Zhang, J., et al. (2020). *Repository: Deuterium and ^{37}Chlorine rich fluids on the surface of Mars: Evidence from the enriched basaltic Shergottite Northwest Africa 8657*. Genève 23 Switzerland: Zenodo. https://doi.org/10.5281/zenodo.3998880

Hu, S., Lin, Y., Zhang, J., Hao, J., Feng, L., Xu, L., et al. (2014). NanoSIMS analyses of apatite and melt inclusions in the GRV 020090 Martian meteorite: Hydrogen isotope evidence for recent past underground hydrothermal activity on Mars. *Geochimica et Cosmochimica Acta*, *140*, 321–333. https://doi.org/10.1016/j.gca.2014.05.008

Hu, S., Lin, Y., Zhang, J., Hao, J., Xing, W., Zhang, T., et al. (2019). Ancient geologic events on Mars revealed by zircons and apatites from the Martian regolith breccia NWA 7034. *Meteoritics & Planetary Science*, *54*(4), 850–879. https://doi.org/10.1111/maps.13256

Hu, S., Lin, Y., Zhang, J., Hao, J., Yamaguchi, A., Zhang, T., et al. (2020). Volatiles in the Martian crust and mantle: Clues from the NWA 6162 shergottite. *Earth and Planetary Science Letters*, *530*, 115902. https://doi.org/10.1016/j.epsl.2019.115902

Hu, S., Lin, Y., Zhang, J., Hao, J., Yang, W., & Deng, L. (2015). Measurements of water content and D/H ratio in apatite and silicate glasses using a NanoSIMS 50L. *Journal of Analytical Atomic Spectrometry*, *30*(4), 967–978. https://doi.org/10.1039/C4JA00417E

Hu, S., Lin, Y., & Zhang, T. (2016). Petrography, mineral chemistry and shock metamorphism of Martian meteorite NWA 8657, 79th Annual Meeting of the Meteoritical Society, #6068.

Irving, A., Kuehner, S., Andreasen, R., Lapen, T., & Chennaoui-Aoudjehane, H. (2015). Petrologic and radiogenic isotopic assessment of olivine-phyric, diabasic and microgabbroic shergottites from Northwest Africa. In *Paper presented at 46th Lunar and Planetary Science Conference, March* (Vol. 46, p. 2290). Houston, USA: Lunar and Planetary Institute.

Jakosky, B. M., Grebowsky, J. M., Luhmann, J. G., Connerney, J., Eparvier, F., Ergun, R., et al. (2015). MAVEN observations of the response of Mars to an interplanetary coronal mass ejection. *Science*, *350*(6261), aad0210. https://doi.org/10.1126/science.aad0210

Jakosky, B. M., Zent, A. P., & Zurek, R. W. (1997). The Mars water cycle: Determining the role of exchange with the regolith. *Icarus*, *130*(1), 87–95. https://doi.org/10.1006/icar.1997.5799

Kim, Y., Konecke, B., Fiege, A., Simon, A., & Becker, U. (2017). An ab-initio study of the energetics and geometry of sulfide, sulfite, and sulfate incorporation into apatite: The thermodynamic basis for using this system as an oxybarometer. *American Mineralogist*, *102*(8), 1646–1656. https://doi.org/10.2138/am-2017-6044

Koike, M., Sano, Y., Takahata, N., Ishida, A., Sugiura, N., & Anand, M. (2016). Combined investigation of H isotopic compositions and U-Pb chronology of young Martian meteorite Larkman Nunatak 06319. *Geochemical Journal*, *50*(5), 363–377. https://doi.org/10.2343/geochemj.2.0424

Konecke, B. A., Fiege, A., Simon, A. C., Linsler, S., & Holtz, F. (2019). An experimental calibration of a sulfur-in-apatite oxybarometer for mafic systems. *Geochimica et Cosmochimica Acta*, *265*, 242–258. https://doi.org/10.1016/j.gca.2019.08.044

Konecke, B. A., Fiege, A., Simon, A. C., Parat, F., & Stechern, A. (2017). Co-variability of S^{6+}, S^{4+}, and S^{2-} in apatite as a function of oxidation state: Implications for a new oxybarometer. *American Mineralogist*, *102*(3), 548–557. https://doi.org/10.2138/am-2017-5907

Kusebauch, C., John, T., Whitehouse, M. J., Klemme, S., & Putnis, A. (2015). Distribution of halogens between fluid and apatite during fluid-mediated replacement processes. *Geochimica et Cosmochimica Acta*, *170*, 225–246. https://doi.org/10.1016/j.gca.2015.08.023

Leshin, L. A. (2000). Insights into Martian water reservoirs from analyses of Martian meteorite QUE94201. *Geophysical Research Letters*, *27*(14), 2017–2020. https://doi.org/10.1029/1999GL008455

Leshin, L. A., Epstein, S., & Stolper, E. M. (1996). Hydrogen isotope geochemistry of SNC meteorites. *Geochimica et Cosmochimica Acta*, *60*(14), 2635–2650. https://doi.org/10.1016/0016-7037(96)00122-6

Leshin, L. A., Mahaffy, P. R., Webster, C. R., Cabane, M., Coll, P., Conrad, P. G., et al. (2013). Volatile, isotope, and organic analysis of Martian fines with the Mars Curiosity rover. *Science*, *341*(6153). https://doi.org/10.1126/science.1238937

Lin, Y., Hu, S., Yamaguchi, A., Zhang, J., Hao, J., & Yang, W. (2019). Global presence of subsurface glacier on Mars evidenced by the correlation between water contents and hydrogen isotopic ratios of Martian meteorites. In *Paper presented at 82nd Annual Meeting of The Meteoritical Society* (Vol. 54, p. 6238). Sapporo, Japan: The Meteoretical Society.

Liu, Y., Chen, Y., Guan, Y., Ma, C., Rossman, G. R., Eiler, J. M., & Zhang, Y. (2018). Impact-melt hygrometer for Mars: The case of shergottite Elephant Moraine (EETA) 79001. *Earth and Planetary Science Letters*, *490*, 206–215. https://doi.org/10.1016/j.epsl.2018.03.019

Mane, P., Hervig, R., Wadhwa, M., Garvie, L. A. J., Balta, J. B., & McSween, H. Y. (2016). Hydrogen isotopic composition of the Martian mantle inferred from the newest Martian meteorite fall, Tissint. *Meteoritics & Planetary Science*, *51*(11), 2073–2091. https://doi.org/10.1111/maps.12717

McCubbin, F., Kaaden, K. E. V., Tartèse, R., Boyce, J. W., Mikhail, S., Whitson, E. S., et al. (2015). Experimental investigation of F, Cl, and OH partitioning between apatite and Fe-rich basaltic melt at 1.0–1.2 GPa and 950–1000°C. *American Mineralogist*, *4779*(8–9), 83–89. https://doi.org/10.2138/am-2015-5233

McCubbin, F. M., & Barnes, J. J. (2019). Origin and abundances of H_2O in the terrestrial planets, Moon, and asteroids. *Earth and Planetary Science Letters*, *526*, 115771. https://doi.org/10.1016/J.Epsl.2019.115771

McCubbin, F. M., Boyce, J. W., Srinivasan, P., Santos, A. R., Elardo, S. M., Filiberto, J., et al. (2016). Heterogeneous distribution of H_2O in the Martian interior: Implications for the abundance of H_2O in depleted and enriched mantle sources. *Meteoritics & Planetary Science*, *51*(11), 2036–2060. https://doi.org/10.1111/maps.12639

McCubbin, F. M., Hauri, E. H., Elardo, S. M., Vander Kaaden, K. E., Wang, J., & Shearer, C. K. (2012). Hydrous melting of the Martian mantle produced both depleted and enriched shergottites. *Geology*, *40*(8), 683–686. https://doi.org/10.1130/g33242.1

McCubbin, F. M., & Jones, R. H. (2015). Extraterrestrial apatite: Planetary geochemistry to astrobiology. *Elements*, *11*(3), 183–188. https://doi.org/10.2113/gselements.11.3.183

McCubbin, F. M., & Nekvasil, H. (2008). Maskelynite-hosted apatite in the Chassigny meteorite: Insights into late-stage magmatic volatile evolution in Martian magmas. *American Mineralogist*, *93*(4), 676–684. https://doi.org/10.2138/am.2008.2558

McCubbin, F. M., Smirnov, A., Nekvasil, H., Wang, J., Hauri, E., & Lindsley, D. H. (2010). Hydrous magmatism on Mars: A source of water for the surface and subsurface during the Amazonian. *Earth and Planetary Science Letters*, *292*(1–2), 132–138. https://doi.org/10.1016/j.epsl.2010.01.028

McCubbin, F. M., Steele, A., Nekvasil, H., Schnieders, A., Rose, T., Fries, M., et al. (2010). Detection of structurally bound hydroxyl in fluorapatite from Apollo Mare basalt 15058, 128 using TOF-SIMS. *American Mineralogist*, *95*(8–9), 1141–1150. https://doi.org/10.2138/am.2010.3448

McCubbin, F. M., Tosca, N. J., Smirnov, A., Nekvasil, H., Steele, A., Fries, M., & Lindsley, D. H. (2009). Hydrothermal jarosite and hematite in a pyroxene-hosted melt inclusion in Martian meteorite Miller Range (MIL) 03346: Implications for magmatic-hydrothermal fluids on Mars. *Geochimica et Cosmochimica Acta*, *73*(16), 4907–4917. https://doi.org/10.1016/j.gca.2009.05.031

McSween, H. Y. Jr., Grove, T. L., Lentz, R. C., Dann, J. C., Holzheid, A. H., Riciputi, L. R., & Ryan, J. G. (2001). Geochemical evidence for magmatic water within Mars from pyroxenes in the Shergotty meteorite. *Nature*, *409*(6819), 487–490. https://doi.org/10.1038/35054011

Nadeau, S. L., Epstein, S., & Stolper, E. (1999). Hydrogen and carbon abundances and isotopic ratios in apatite from alkaline intrusive complexes, with a focus on carbonatites. *Geochimica et Cosmochimica Acta*, *63*(11–12), 1837–1851. https://doi.org/10.1016/S0016-7037(99)00057-5

Owen, T., Maillard, J. P., de Bergh, C., & Lutz, B. L. (1988). Deuterium on Mars: The abundance of HDO and the value of D/H. *Science*, *240*(4860), 1767. https://doi.org/10.1126/science.240.4860.1767

Peslier, A. H., Hervig, R., Yang, S., Humayun, M., Barnes, J. J., Irving, A. J., & Brandon, A. D. (2019). Determination of the water content and D/H ratio of the Martian mantle by unraveling degassing and crystallization effects in nakhlites. *Geochimica et Cosmochimica Acta*, *266*, 382–415. https://doi.org/10.1016/j.gca.2019.04.023

Robert, F., Gautier, D., & Dubrulle, B. (2000). The solar system D/H ratio: Observations and theories. *Space Science Reviews*, *92*(1/2), 201–224. https://doi.org/10.1023/a:1005291127595

Ross, D., Ito, M., Hervig, R., Rao, M., & Nyquist, L. (2011). Recognizing the effects of terrestrial contamination on D/H ratios in shergottite phosphates. In *Paper presented at 42nd Lunar and Planetary Science Conference* (Vol. 42 p. 1920). Houston, USA: Lunar and Planetary Institute.

Sarafian, A. R., Hauri, E. H., McCubbin, F. M., Lapen, T. J., Berger, E. L., Nielsen, S. G., et al. (2017a). Early accretion of water and volatile elements to the inner solar system: Evidence from angrites. *Philosophical Transactions. Series A, Mathematical, Physical, and Engineering Sciences*, *375*(2094), 20160209. https://doi.org/10.1098/rsta.2016.0209

Sarafian, A. R., John, T., Roszjar, J., & Whitehouse, M. J. (2017b). Chlorine and hydrogen degassing in Vesta's magma ocean. *Earth and Planetary Science Letters*, *459*, 311–319. https://doi.org/10.1016/j.epsl.2016.10.029

Sautter, V., Jambon, A., & Boudouma, O. (2006). Cl-amphibole in the nakhlite MIL 03346: Evidence for sediment contamination in a Martian meteorite. *Earth and Planetary Science Letters*, *252*(1–2), 45–55. https://doi.org/10.1016/j.epsl.2006.09.024

Sharp, Z., Williams, J., Shearer, C., Agee, C., & McKeegan, K. (2016). The chlorine isotope composition of Martian meteorites 2. Implications for the early solar system and the formation of Mars. *Meteoritics & Planetary Science*, *51*(11), 2111–2126. https://doi.org/10.1111/maps.12591

Sharp, Z. D., McCubbin, F. M., & Shearer, C. K. (2013). A hydrogen-based oxidation mechanism relevant to planetary formation. *Earth and Planetary Science Letters*, *380*, 88–97. https://doi.org/10.1016/j.epsl.2013.08.015

Sharp, Z. D., Shearer, C. K., McKeegan, K. D., Barnes, J. D., & Wang, Y. Q. (2010). The chlorine isotope coomposition of the Moon and implications for an anhydrous mantle. *Science*, *329*, 1050–1053. https://doi.org/10.1126/science.1192606

Shearer, C. K., Messenger, S., Sharp, Z. D., Burger, P. V., Nguyen, A. N., & McCubbin, F. M. (2018). Distinct chlorine isotopic reservoirs on Mars. Implications for character, extent and relative timing of crustal interactions with mantle-derived magmas, evolution of the Martian atmosphere, and the building blocks of an early Mars. *Geochimica et Cosmochimica Acta*, *234*, 24–36. https://doi.org/10.1016/j.gca.2018.04.034

Stephant, A., Garvie, L. A. J., Mane, P., Hervig, R., & Wadhwa, M. (2018). Terrestrial exposure of a fresh Martian meteorite causes rapid changes in hydrogen isotopes and water concentrations. *Scientific Reports*, *8*(1), 12385. https://doi.org/10.1038/s41598-018-30807-w

Sugiura, N., & Hoshino, H. (2000). Hydrogen-isotopic compositions in Allan Hills 84001 and the evolution of the Martian atmosphere. *Meteoritics & Planetary Science*, *35*(2), 373–380. https://doi.org/10.1111/j.1945-5100.2000.tb01783.x

Tartèse, R., Anand, M., & Franchi, I. A. (2019). H and Cl isotope characteristics of indigenous and late hydrothermal fluids on the differentiated asteroidal parent body of Grave Nunataks 06128. *Geochimica et Cosmochimica Acta*, *266*, 529–543. https://doi.org/10.1016/j.gca.2019.01.024

Tartèse, R., Anand, M., Joy, K. H., & Franchi, I. A. (2014). H and Cl isotope systematics of apatite in brecciated lunar meteorites Northwest Africa 4472, Northwest Africa 773, Sayh al Uhaymir 169, and Kalahari 009. *Meteoritics & Planetary Science*, *49*(12), 2266–2289. https://doi.org/10.1111/maps.12398

Usui, T., Alexander, C. M. D., Wang, J., Simon, J. I., & Jones, J. H. (2012). Origin of water and mantle-crust interactions on Mars inferred from hydrogen isotopes and volatile element abundances of olivine-hosted melt inclusions of primitive shergottites. *Earth and Planetary Science Letters*, *357-358*, 119–129. https://doi.org/10.1016/j.epsl.2012.09.008

Usui, T., Alexander, C. M. O. D., Wang, J., Simon, J. I., & Jones, J. H. (2015). Meteoritic evidence for a previously unrecognized hydrogen reservoir on Mars. *Earth and Planetary Science Letters*, *410*, 140–151. https://doi.org/10.1016/j.epsl.2014.11.022

Villanueva, G. L., Mumma, M. J., Novak, R. E., Kaufl, H. U., Hartogh, P., Encrenaz, T., et al. (2015). Strong water isotopic anomalies in the Martian atmosphere: Probing current and ancient reservoirs. *Science*, *348*(6231), 218–221. https://doi.org/10.1126/science.aaa3630

Watson, L. L., Hutcheon, I. D., Epstein, S., & Stolper, E. M. (1994). Water on Mars: Clues from deuterium/hydrogen and water contents of hydrous phases in SNC meteorites. *Science*, *265*(5168), 86–90. https://doi.org/10.1126/science.265.5168.86

Webster, C. R., Mahaffy, P. R., Flesch, G. J., Niles, P. B., Jones, J. H., Leshin, L. A., et al. (2013). Isotope ratios of H, C, and O in CO_2 and H_2O of the Martian atmosphere. *Science*, *341*(6143), 260–263. https://doi.org/10.1126/science.1237961

Wei, Y., Pu, Z., Zong, Q., Wan, W., Ren, Z., Fraenz, M., et al. (2014). Oxygen escape from the Earth during geomagnetic reversals: Implications to mass extinction. *Earth and Planetary Science Letters*, *394*, 94–98. https://doi.org/10.1016/j.epsl.2014.03.018

Williams, J. T., Shearer, C. K., Sharp, Z. D., Burger, P. V., McCubbin, F. M., Santos, A. R., et al. (2016). The chlorine isotopic composition of Martian meteorites 1: Chlorine isotope composition of Martian mantle and crustal reservoirs and their interactions. *Meteoritics & Planetary Science*, *51*(11), 2092–2110. https://doi.org/10.1111/maps.12647

Zhang, Y., & Behrens, H. (2000). H_2O diffusion in rhyolitic melts and glasses. *Chemical Geology*, *169*(1–2), 243–262. https://doi.org/10.1016/s0009-2541(99)00231-4

Zhu, C., & Sverjensky, D. A. (1991). Partitioning of F-Cl-OH between minerals and hydrothermal fluids. *Geochimica et Cosmochimica Acta*, *55*(7), 1837–1858. https://doi.org/10.1016/0016-7037(91)90028-4